Ammonia detection by use of quartz-enhanced photoacoustic spectroscopy with a near-IR telecommunication diode laser

Anatoliy A. Kosterev and Frank K. Tittel

A gas sensor based on quartz-enhanced photoacoustic detection and a fiber-coupled telecommunication distributed-feedback diode laser was designed and characterized for trace NH_3 monitoring at a 1.53-μm wavelength (overtone absorption region). Signal and noise dependence on gas pressure were studied to optimize sensor performance. The ammonia concentration resulting in a noise-equivalent signal was found to be 0.65 parts per million by volume with 38-mW optical excitation power and a lock-in amplifier time constant of 1 s. This corresponds to a normalized absorption sensitivity of 7.2×10^{-9} cm^{-1} W/Hz$^{1/2}$, comparable with detection sensitivity achieved in conventional photoacoustic spectroscopy. The sensor architecture can be the basis for a portable gas analyzer. © 2004 Optical Society of America
    OCIS codes: 300.6430, 280.3420.

1. Introduction

Trace ammonia quantification in the gas phase at different concentration levels is required in diverse areas of applications such as industrial process control, automotive exhaust analysis, medical diagnostics, and environmental monitoring. One specific application that requires ammonia detection at a few parts per million by volume (ppmv) is the identification of leaks in industrial refrigeration systems. Industrial use requires a robust and preferably portable sensor that is immune to harsh environmental conditions. Telecommunication laser diodes are well-suited spectroscopic sources for such applications. It was shown previously that both direct absorption spectroscopy[1] and photoacoustic spectroscopy (PAS)[2] in the near-IR region can deliver sufficient sensitivity and selectivity. Direct absorption measurements, however, require a 36-m-pathlength multipass cell and balanced detection, making the sensor architecture too complex for many field deployable applications. PAS allows the replacement of a multipass cell with a compact and less-expensive photoacoustic cell, but this approach can suffer from background acoustic noise and sampled gas-flow noise. These shortcomings of PAS can be eliminated if the recently reported quartz-enhanced PAS (QEPAS)[3] technique is applied. The basic concept of QEPAS is the use of a regular clock-frequency stabilization element, a quartz tuning fork (TF) as a resonant transducer for the acoustic signal. The advantages of such a transducer are its very high Q factor ($Q > 10\,000$) resulting in long accumulation times of the acoustic energy, a virtual immunity to the ambient acoustic noise on account of being an acoustic quadrupole, and its very small size (5 mm × 1.5 mm × 0.3 mm typical dimensions). In addition, the QEPAS approach makes a gas cell optional. If such a cell is still desirable for gas sample isolation, it can be made as small as a few cubic millimeters in volume and of arbitrary shape.

The QEPAS sensor configuration is similar to that reported in earlier publications[3,4] and is shown in Fig. 1. It is based on a $2f$ wavelength-modulation photoacoustic-detection approach. A fiber-coupled distributed-feedback telecommunication diode laser model NLK1C5J1AA; NTT Electronics Corp., Tokyo, Japan) served as an excitation source for generating a photoacoustic sound. The dc component of the laser current determines its central wavelength, whereas the sinusoidal ac component produces the wavelength modulation. A notebook personal computer with a data acquisition card (DAQCard 6062E; National Instruments, Austin, Texas) and LABVIEW-based software was used to collect data and control the dc voltage applied to the laser driver, as well as

The authors are with the Rice Quantum Institute, Rice University, Houston, Texas 77251-1892. A. Kosterev's e-mail address is akoster@rice.edu.
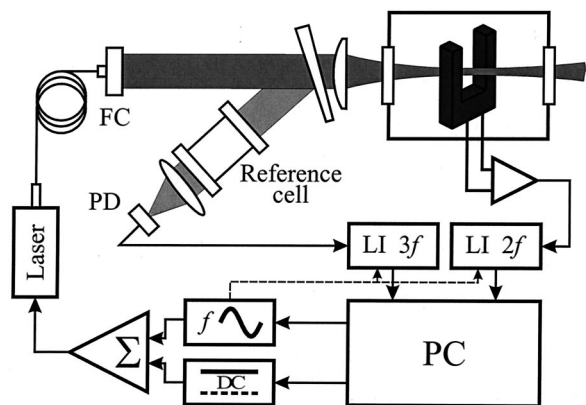
Fig. 1. Schematic of the QEPAS-based laboratory ammonia sensor. FC, fiber collimator; PD, photodiode. LI 3*f* and 2*f* are lock-in amplifiers set to detect respectively third- and second-harmonic components with respect to the reference frequency. The dashed line from the function generator indicates that the generator is providing a reference to the LIs. The laser driver and the temperature controller are not shown.
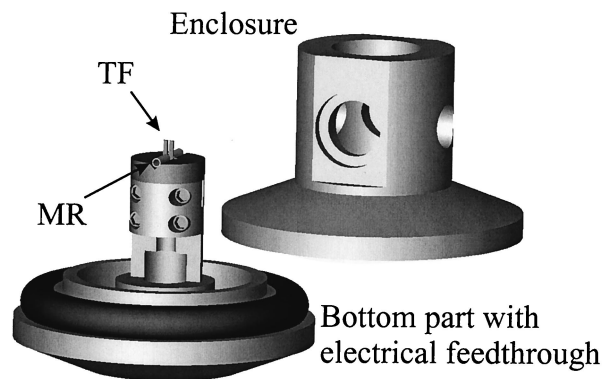

Fig. 2. Sketch of the QEPAS gas cell. MR, microresonator; TF, quartz tuning fork. All parts are drawn to scale except for the MR, whose actual size is smaller and its position is closer to the TF opening. The outer diameter of the flanges is 40 mm. The top opening in the enclosing flange is for a pressure transducer, right and left openings are for the gas input and output, and front and back are for optical windows.

the ac component produced by a function generator. The piezoelectric current generated by the TF was converted to a voltage by means of a transimpedance preamplifier. Prior to each run of experiments, the TF resonant frequency and Q factor were measured by applying a harmonic voltage excitation to the TF and recording the current while the excitation frequency was scanned. For the actual ammonia detection, the laser modulation frequency f was set to half of the resonant frequency of the TF, and the TF generated signal was rectified at $2f$ frequency by means of a lock-in amplifier. The laser wavelength can be either scanned to acquire $2f$ spectra, or locked to a selected absorption line for continuous concentration monitoring. Wavelength locking was performed with a common $3f$ approach. Namely, a small fraction of the laser radiation was directed through the reference gas cell containing NH_3 in nitrogen at such a concentration to ensure 5% to 20% peak absorption at the target wavelength. A total pressure in the reference cell was ~2 times higher than the pressure in the TF gas cell. The signal from a photodiode PD (Fig. 1) was demodulated at $3f$ frequency. The $3f$ component crossed zero at the line center and was approximately linear with detuning if the detuning is sufficiently small, which allows to use this signal as feedback in the wavelength stabilization loop. We found that a simple proportional regulation of the dc laser current was sufficient for long-term frequency stabilization of the diode laser.

A TF with a resonance frequency $f_0 \sim 32\,760$ Hz (most common available commercially) was used as a microphone. To enhance the photoacoustic pressure, an acoustic microresonator was added. The microresonator consists of two glass tubes, each 2.45 mm long with a 0.32-mm inner diameter, aligned with the laser beam perpendicular to the TF plane. The combined tube length is made to be equal to half of the sound wavelength at f_0 to satisfy the resonant

condition.[5] Laser radiation was focused between the TF prongs with a 36-mm-focal-length lens. The laser wavelength was modulated at $f = f_0/2$ frequency with an amplitude sufficient for spanning the target absorption line. The design of the optical gas cell with a TF is depicted in Fig. 2. This gas cell was fabricated from a standard NW25 vacuum flange and equipped with two sapphire windows, two gas throughputs, and a piezoresistive pressure transducer. The estimated cell volume of this particular design is ~1 cm^3.

The absorption line selection for NH_3 detection was based on data reported by Webber *et al.*[6] A NH_3 line at 6528.76 cm^{-1} was chosen as the target. At pressures $P \geq 500$ Torr this line merges with its weaker neighbor at 6528.89 cm^{-1}. Simulated absorption spectra are shown in Fig. 3(a). The laser power delivered to the TF at the target wavelength was measured to be 38 mW. A permeation-tube-based gas-standards generator (model 491 M; Kin-Tek, La Marque, Texas) was used to generate calibrated trace concentrations of NH_3 in pure N_2. All of the measurements were performed in gas flow to reduce adsorption–desorption effects, typically 50 SCCM (cubic centimeters per minute at STP) N_2 mass-flow. Sample QEPAS spectra of 50 ppmv NH_3:N_2 are shown in Fig. 3(b).

The amplitude of the detected QEPAS signal is determined by the following factors:

(1) Peak intensity of the absorption line,
(2) Vibrational–translational energy transfer rate of the molecule,
(3) The TF Q factor,
(4) An enhancement factor of the microresonator,
(5) Laser modulation depth.

Factors (1)–(4) are pressure dependent. Laser wavelength modulation [factor (5)] must match the pressure-dependent absorption linewidth [the high-
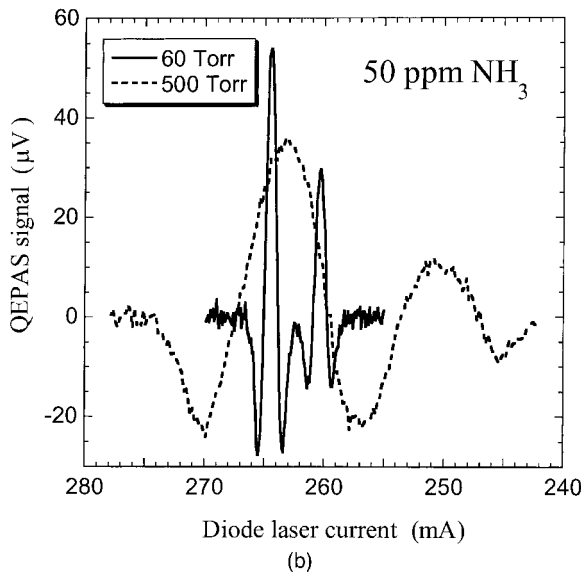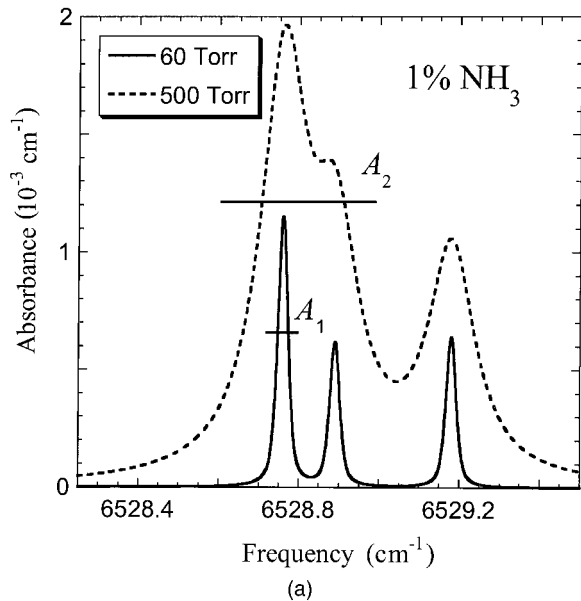
(a)

(b)

Fig. 3. (a) Simulated ammonia absorption based on spectroscopic parameters from Ref. 6. The horizontal lines A_1 and A_2 show peak-to-peak wavelength modulation resulting in the highest QEPAS signal at 60 Torr and 500 Torr, respectively. (b) QEPAS spectra of the same lines acquired at a 50-ppmv NH_3 concentration, optimum wavelength modulation, and a 0.3-s lock-in amplifier time constant.

est $2f$ signal is achieved when the modulation width is close to the absorption linewidth, as shown in Fig. 3(a)]. Therefore, to optimize the sensor performance, both the gas pressure and the wavelength-modulation depth must be appropriately chosen. In this work the QEPAS signal corresponding to the peak absorption was mapped as a function of gas pressure and laser current modulation depth (Fig. 4). The measurements were carried out with a 50-ppmv NH_3 in N_2 mixture, as described above. It is evident that the highest signal is observed at 60 Torr. The signal amplitude decreases at higher pressures until
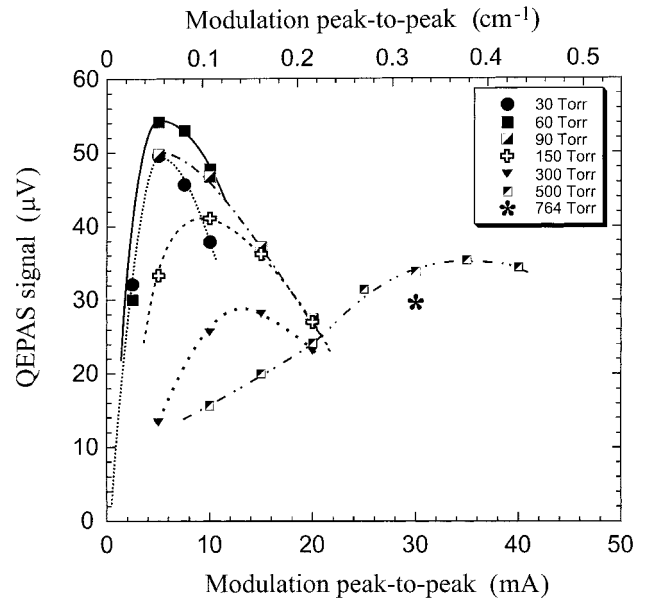

Fig. 4. QEPAS signal at the transimpedance preamplifier output corresponding to the peak NH_3 absorption near 6528.8 cm^{-1} for different gas pressures and laser current modulation depth. All measurements were performed at a 50-ppmv NH_3 in N_2 mixture and a 40 SCCM gas mass flow. (SCCM denotes cubic centimeters per minute at STP.)

the absorption lines start to merge at 500 Torr. The atmospheric pressure (764 Torr) signal is ~10% weaker than the signal at 500 Torr.

The sensitivity is determined by the signal-to-noise ratio (SNR), and it was verified in several experimental tests that the observed QEPAS noise is equal to the theoretical thermal noise of the TF at its resonance frequency[7]:

$$\frac{(\langle V_N^2 \rangle)^{1/2}}{\sqrt{\Delta f}} = R_{\text{fb}} \left(\frac{4k_B T}{R} \right)^{1/2}, \qquad (1)$$

$$R = \frac{1}{Q} \sqrt{\frac{L}{C}}, \qquad (2)$$

where $(\langle V_N^2 \rangle)^{1/2}$ is the rms voltage noise observed at the transimpedance amplifier output; Δf is the detection bandwidth $\{\Delta f = [1/2\pi\tau]$, where τ is the lock-in amplifier time constant$\}$; R_{fb} is the amplifier feedback resistor; T is the TF temperature; and R, L, and C are the electrical parameters of the TF when it is represented by the equivalent serial resonant circuit. From Eqs. (1) and (2), it follows that the noise is directly proportional to $(Q)^{1/2}$. The photoacoustic signal is directly proportional to Q. Thus the SNR increases proportionally to $(Q)^{1/2}$ if all other parameters are kept constant. In the gas pressure range 30–500 Torr the Q factor was found to change from 31 000 to 12 600. The measured SNR at optimum laser current modulation depth is shown in Fig. 5 as a function of gas pressure. It is evident that the sensitivity at atmospheric pressure is almost the same as at 60 Torr, regardless of the Q-factor de-
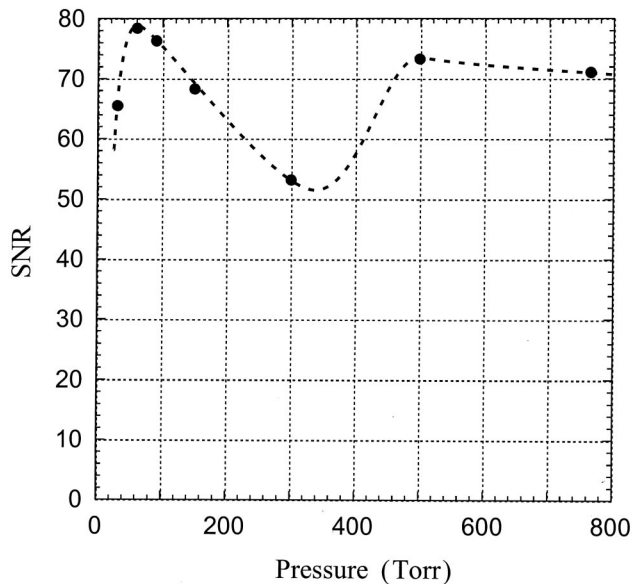
Fig. 5. SNR at different pressures with optimum laser current modulation depth for each pressure for a 50-ppmv NH_3 in N_2 mixture and a 1-s time constant. The SNR decrease in the pressure range 60–250 Torr is due to a decreasing Q factor of the TF, and the secondary rise at 500 Torr is caused by a merging of two closely spaced ammonia absorption lines.

crease. This effect is caused by the merging of two absorption lines, as shown in Fig. 3(a). Thus the QEPAS sensor can operate with almost equal performance at 60 Torr if high spectral resolution or low mass flow of the gas is required, or at ambient atmospheric pressure to eliminate the use of vacuum components.

The linearity and the sensitivity of the sensor were verified by measuring its response to the changing NH_3 concentration in N_2 flow of 40 sccm. The measurements were performed at 60 Torr pressure in the TF cell and optimum modulation (6 mA peak to peak, or 0.065 cm^{-1}). The laser wavelength was locked to the center of the 6528.76-cm^{-1} NH_3 absorption line. The results of repetitive measurements made every 1.5 s are plotted in Fig. 6(a). The phase of the detected signal was found to be independent of the NH_3 concentration. The scatter of consecutive measurements at a certain concentration level also did not depend on the concentration and was in agreement with Eq. (1). Based on these data, the NH_3 concentration that would result in noise-equivalent (1σ) sensor readings is 0.65 ppmv, assuming a 1-s lock-in amplifier time constant, 60-Torr gas pressure and 38-mW optical excitation power. The corresponding absorption coefficient normalized to optical power and detection bandwidth is $k = 7.2 \times 10^{-9}$ cm^{-1} W/Hz$^{1/2}$. This normalized sensitivity is only 4 or 5 times lower than the best results reported for conventional wavelength-modulation PAS[2,8] and somewhat better than that reported for amplitude-modulation PAS.[9] As compared with the first QEPAS publication[3] in which CH_4 detection was reported, this number shows an improvement by a factor of 16. The main reason
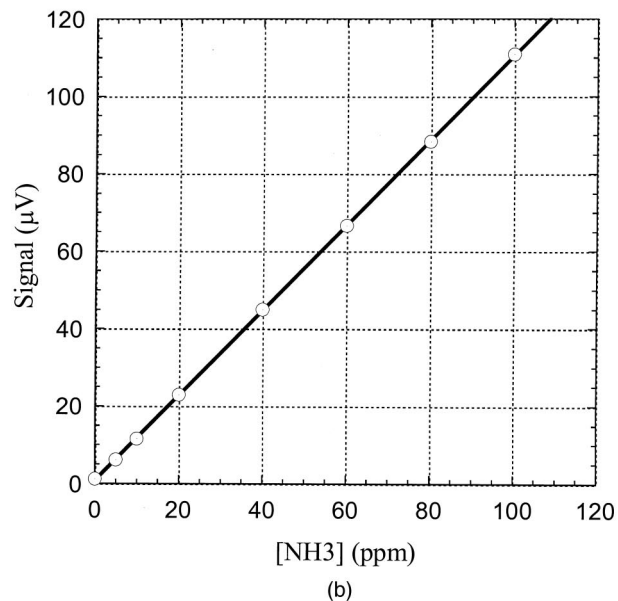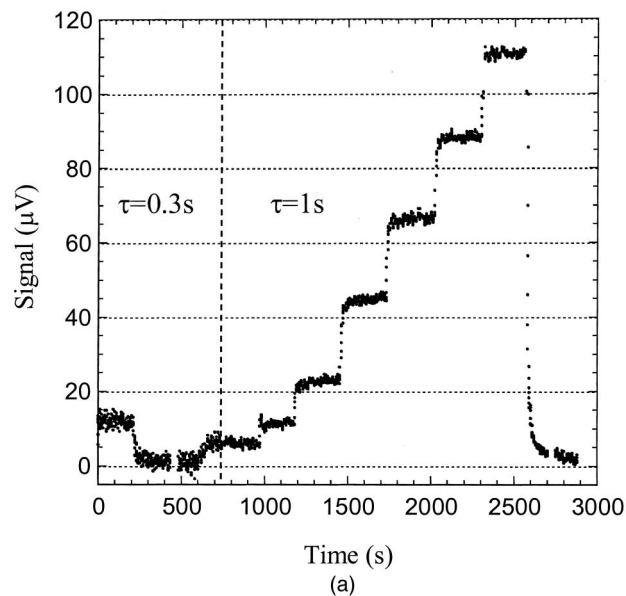

(a)

[NH3] (ppm)

(b)

Fig. 6. (a) QEPAS signal (transimpedance preamplifier output) repetitively recorded while the NH_3 concentration was varied by a changing of the carrier gas flow in the gas standards generator. (b) Same data averaged (90 most-recent measurements out of 180 at each carrier gas mass-flow rate) and plotted as a function of NH_3 concentration based on the calibration of the gas standards generator.

for this is the faster operational amplifier used in the transimpedance preamplifier circuit. Other enhancement factors include a better microresonator design and possibly a faster V-T transfer from NH_3 than from CH_4 vibrations.

The plot in Fig. 6(b) is a representation of the same measurements after the last 90 sensor readings of each concentration step are averaged. This plot confirms the linearity of the sensor response to concentration. These measurements were performed in a dynamic range of only ~100 because of the gas-

standards generator limitations. Our previous experiments with acetylene proved the sensor linearity within the dynamic range of ~1000, and the TF is known to be a linear displacement-to-charge transducer with a dynamic range of $>10^7$. Both zero intercept and the readings in the "zero gas" mode of the gas-standards generator indicate the presence of ~1 ppmv of NH_3. Absence of such a signal for ambient air measurements confirms that this is not a systematic instrumental error but the real residual NH_3 concentration in the "zero gas."

In conclusion, it was demonstrated that the QEPAS approach can be used for trace-gas detection with commercially available near-IR lasers. The QEPAS sensitivity is in the same range as the sensitivity of conventional PAS with the added advantages of noise immunity and an ultrasmall sample volume. These features potentially allow the conversion of a laboratory setup into a portable device for field applications. Considerable gain in performance is expected if custom or modified TFs with lower resonant frequency are used, because the photoacoustic signal is inversely proportional to the modulation frequency. The technology may also benefit from a better design and tighter tolerances of the acoustic microresonator. QEPAS response is directly proportional to both the laser power and the absorption coefficient. Therefore the concentration detection limits can be much lower if either higher power sources are used (for example, fiber-amplified diode lasers) or fundamental molecular absorption bands are accessed.[10]

References

1. R. Claps, F. V. Englich, D. P. Leleux, D. Richter, F. K. Tittel, and R. F. Curl, "Ammonia detection by use of near-infrared diode-laser-based overtone spectroscopy," Appl. Opt. **40,** 4387–4394 (2001).
2. A. Schmohl, A. Miklós, and P. Hess, "Detection of ammonia by photoacoustic spectroscopy with semiconductor lasers," Appl. Opt. **41,** 1815–1823 (2002).
3. A. A. Kosterev, Yu. A. Bakhirkin, R. F. Curl, and F. K. Tittel, "Quartz-enhanced photoacoustic spectroscopy," Opt. Lett. **27,** 1902–1904 (2002).
4. D. Weidmann, A. A. Kosterev, F. K. Tittel, N. Ryan, and D. McDonald, "Application of a widely electrically tunable diode laser to chemical gas sensing with quartz-enhanced photoacoustic spectroscopy," Opt. Lett. **29,** 1837–1839 (2004).
5. A. Miklós, P. Hess, and Z. Bozóki, "Application of acoustic resonators in photoacoustic trace gas analysis and metrology," Rev. Sci. Instr. **72,** 1937–1955 (2001).
6. M. E. Webber, D. S. Baer, and R. K. Hanson, "Ammonia monitoring near 1.5 μm with diode-laser absorption sensors," Appl. Opt. **40,** 2031–2042 (2001).
7. R. D. Grober, J. Acimovic, J. Schuck, D. Hessman, P. J. Kindlemann, J. Hespanha, A. S. Morse, K. Karrai, I. Tiemann, and S. Manus, "Fundamental limits to force detection using quartz tuning forks," Rev. Sci. Instrum. **71,** 2776–2780 (2000).
8. M. E. Webber, M. Pushkarsky, and C. K. N. Patel, "Fiber-amplifier-enhanced photoacoustic spectroscopy with near-infrared tunable diode lasers," Appl. Opt. **42,** 2119–2126 (2003).
9. M. B. Pushkarsky, M. E. Webber, and C. K. N. Patel, "Ultrasensitive ambient ammonia detection using CO_2-laser-based photoacoustic spectroscopy," Appl. Phys. B **77,** 381–385 (2003).
10. A. A. Kosterev, Y. A. Bakhirkin, and F. K. Tittel, "Ultrasensitive gas detection by quartz-enhanced photoacoustic spectroscopy in the fundamental molecular absorption bands region," Appl. Phys. B, 10.1007/s00340-004-1619-y.